Instrument Design Document
Subsystem: Optics
Status: V5.2
Date: November 22, 2010
Document custodian: Jason Koglin

1. Configuration Definition and Functional Description

Two NuSTAR optics modules focus X-rays over a broad energy range (6-80 keV) onto their respective CdZnTe detectors. Segmented, multilayer-coated mirrors are built up from a titanium base mandrel using graphite spacers and epoxy. The inner layers will have sextant segmentation (i.e. ~60 degree azimuth span mirrors) and the outer layer will have twelvetant segmentation (i.e. ~30 degree azimuth span mirrors). The transition from sextant to twelvetant mirrors will be made using three layers of substrates that will be multilayer coated and are expected to have good quality figure and thus may potentially provide extra effective area (over the baseline of 130 reflective layers). They will serve as an intermediate mandrel that will support the change in spacer configuration from the sextant to twelvetant geometry and will also provide overall structural support by tying together the sector sections. A skeletal outer mandrel will join the upper and lower halves of the optic. The optics modules will be co-aligned and mounted via Aluminum spider supports to canisters at the end of the extendable mast, which will be deployed after reaching orbit. The spider supports are designed to completely obscure the region between adjacent sextant segments. An illustration of a complete optics module is shown in Figure 1.

2. Coordinate System definition

The optical axis is well defined by our assembly approach in which each mirror segment is mounted to graphite spacers that are precisely machined to the correct angle and radius, which are measured with respect to fixed points on the inner optic mandrel. The optical axis will be confirmed with X-ray calibration measurements. Mechanical alignment points will be used to define a mechanical boresight that is co-aligned with the optical axis. While the exact rotational alignment about the optical axis is not critical to the optical imaging performance, it will be well defined based on the mechanical alignment points.

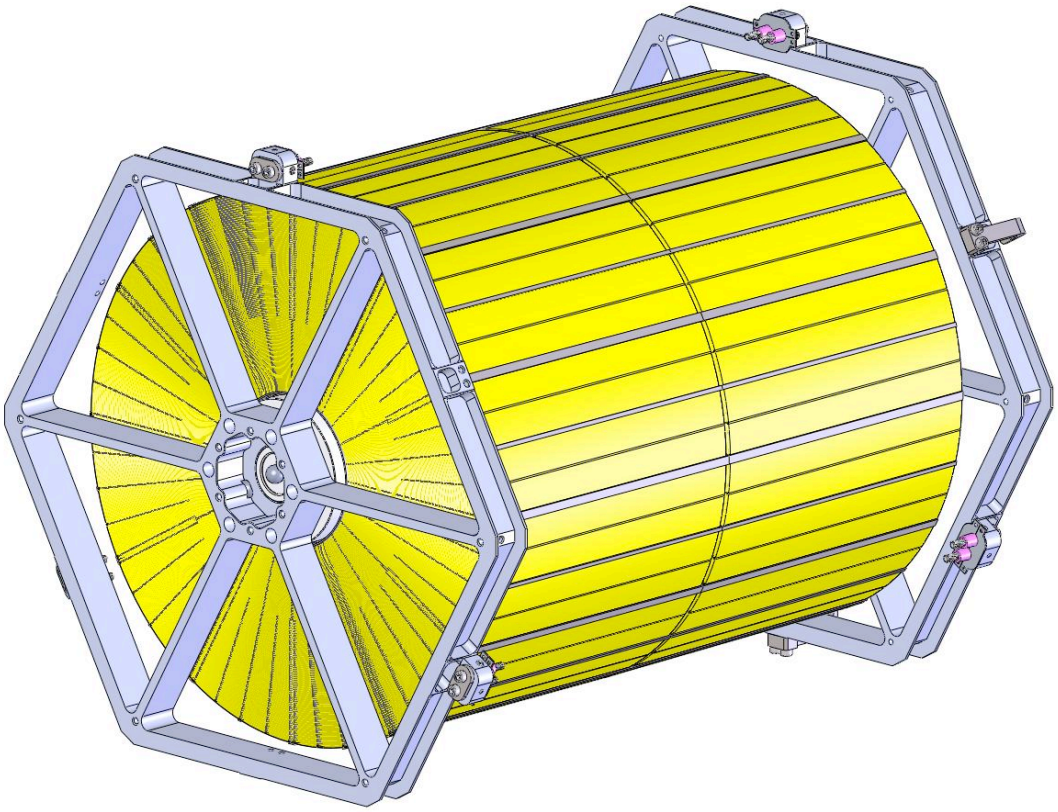

Figure 1: NuSTAR optics with spider mounts

3. Mechanical Description

The NuSTAR optics design is based on a conical approximation to a Wolter-I telescope. True Wolter-I telescopes are comprised of concentric shells of primary (parabolic) and secondary (hyperbolic) mirrors. They have been successfully used for the soft (~0.1-10 keV) band starting with the Einstein Observatory to the Chandra and XMM-Newton Observatories of today. NuSTAR is designed for energies between 6 to 80 keV. To achieve high reflectivity at these energies, the nominal graze angles of the mirrors must be less than for softer X-rays; thus NuSTAR will have a relatively long focal length (F = 10.150 m, defined as the length from the midpoint between the primary and secondary mirrors to the focal plane detector). Further, NuSTAR will employ depth graded multilayers to achieve enhanced, wide-band reflectivity (see Multilayer Instrument Design Document). The long focal length, together with the NuSTAR image performance requirement of 43" half power diameter (HPD, the focal plane diameter within which half of the focused photons are enclosed) means that the primary and secondary mirrors can be approximated to be the surfaces of cones with minimal impact to the image performance. This significantly simplifies the optics design and manufacturing. The general telescope design parameters are given in Table 1.

3.1. Layer Geometry

NuStar will have two optics modules, each composed of 133 sets of conic shells, 3 of which will serve as the intermediate mandrel. The upper conic shell forms an angle α with respect to the optics axis, while the lower shell forms an angle 3α with respect to the

optics axis. In this way, on-axis photons are reflected from the lower shell surface by an angle 4α (for perfect mirrors).

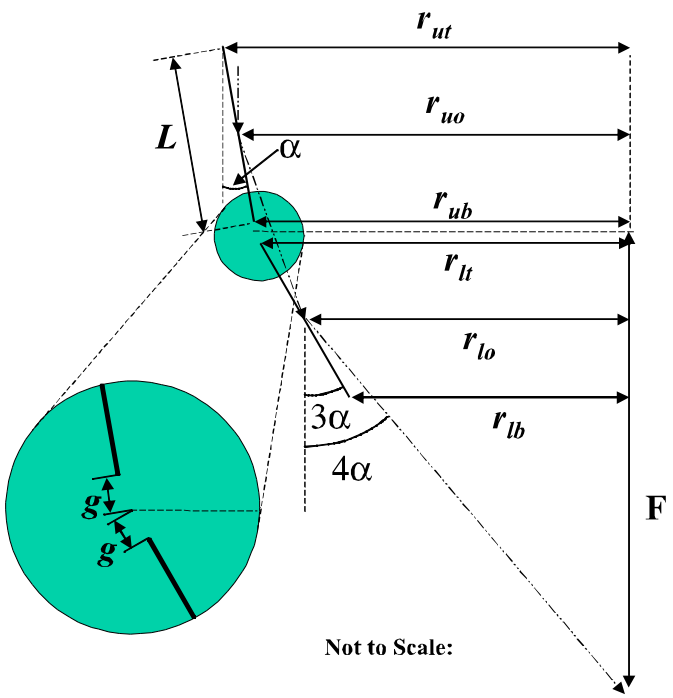

Figure 2: Optics design. F is the focal length, L is the shell length, α is the graze angle, g is the gap between the upper and lower shells and the radius is identified at several points.

Since the lengths of the shells, L = 225 mm, is relatively small compared to the focal length, these conic shells are a good approximation to the parabolic and hyperbolic form for true Wolter I optics. Further, the angle α is small enough that the small angle approximation, $\sin(\alpha) = \tan(\alpha) = \alpha$, may be used for all calculations (at most it effects the calculations of the shell radii by just over 1 ppm). In order to minimize the conic approximation aberration, the relationship between the angle α and the radius to the center of the upper shell, r_{uo}, is defined to be

$$r_{uo} = 4\alpha F,$$

where F is the focal length as shown in Figure 2. To calculate the positions for all 130 sets of shells, it is convenient to use the top of the upper shell,

$$r_{ut} = r_{uo} + \alpha L/2.$$

The angle α can then be written as

$$\alpha = (r_{ut})/(4F+L/2). \qquad (1)$$

The radii at other points of each layer are then given by

$$r_{ub} = r_{ut} - \alpha L$$

$$r_{lt} = r_{ut} - \alpha(L + 4g)$$

$$r_{lb} = r_{ut} - 4\alpha(L+g)$$

where g = 2 mm is the distance from the intersection of the upper and lower surfaces extended to both the upper bottom shell edge and the lower top shell edge (see Figure 2). A radius dependent gap between each shell is used such that the difference in radii r_{ut} between consecutive shells i and i-1 (where the shell i-1 has a smaller radius than the shell i) is

$$\Delta r_{ut}(i,i\text{-}1) = \alpha_i L f_{gap} + t_{glass} , \quad (2)$$

where f_{gap} = 1.3313 is the variable gap parameter and t_{glass} is the glass substrate thickness. Combining the last two equations and solving for a

$$\alpha_i = (r_{ut,i\text{-}1} + t_{glass})/(4F+L/2-Lf_{gap})$$

so that

$$r_{ut,i} = (r_{ut,i\text{-}1} + t_{glass})\{1 + [(4F)/(Lf_{gap})+1/(2f_{gap})-1]^{-1}\}. \quad (3)$$

3.2. Mirror Segment Geometry

Each complete shell is comprised of individual segmented mirrors. The segmentation of the mirrors will change midway through the optic. The parameters for the inner and outer sets of shells are given in Table 2. The inner 65 shells will be built directly off the inner base mandrel with the upper and lower shells, each comprised of six (n_{segs} = 6), L = 225 mm long mirror segments made of t_{glass} = 0.21 mm thick, D263 glass substrates with multilayer coatings. Each mirror segment will be supported by five ($n_{spacers}$ = 5), w_{spacer} = 1.2 mm wide graphite spacers that run the full axial length of the mirror segment (i.e., 225 mm long).

The transition from sextant to twelvetant mirrors will be made using three layers of substrates that will be multilayer coated and are expected to have good quality figure and thus may potentially provide extra effective area (over the baseline of 130 reflective layers). Based on an engineering analysis of stress at this interface, all three of these layers will be the standard thickness (0.21 mm) glass. These layers (66-68) will serve as an intermediate mandrel that will support the change in spacer configuration from the sextant to twelvetant geometry and will also provide overall structural support by tying together the sector sections.

The next 65 shells are comprised of twelve (n_{segs} = 12), 225 mm long mirror segments also made of 0.21 mm thick, D263 glass. Each mirror segment will also be supported by five ($n_{spacers}$ = 5), w_{spacer} = 1.2 mm wide graphite spacers that run the full axial length of the mirror segment (i.e., 225 mm long).

The mirror segments will be sized to allow for a w_{gap} = 1.0 mm average gap between adjacent segments such that the arclength is given by

$$S = 2\pi r/n_{segs} - w_{gap}, \quad (4)$$

where r is the radius of the segment. The cut size of each mirror segment is thus defined by this equation with top (bottom) radius of each upper segment given by r_{ut} (r_{ub}) and the top (bottom) radius of each lower segment given by r_{lt} (r_{lb}) as defined by the equations in Section 3.1. These cut dimensions for the inner (outer) 65 layers are detailed in Table 8 (Table 9). The cut dimensions for the intermediate transition layers (66-69) are detailed in Table 7.

The 'skeletal' outer mandrel will join the upper and lower halves of the optic and tie the twelvetant sectors together azimuthally. The baseline engineering design is to tie the twelvetant sectors together at their adjacent outside spacers using strips of Titanium (8 mm wide and 1 mm thick) along the entire length of the optic (454 mm long from the top of the upper shell to the bottom of the lower shell).

Based on these design details, mass estimates are given in Table 3. The cut shell geometries are posted on the NuSTAR twiki as NuSTAR_CutShellGeometryV20.txt.

3.3. Spacer Configuration and Obscuration

The spacers are w_{spacer} = 1.2 mm wide, except for up to the five innermost layers (1-5) where the spacers will be w_{spacer} = 1.6 mm wide since this is the area of highest stress concentration. On average, a small epoxy fillet w_{fillet} = 1.0 mm wide (i.e. 0.5 mm average on each side) around the spacer will cause added obscuration for each spacer. Thus, on average, each spacer is expected to obscure 2.2 mm of the segment. The aluminum spider supports that connect the inner optic mandrel to the canisters at the end of the spacecraft's extendable mast are designed to divide the optic into sextant sectors that align with the sextant segmented mirrors. In this way, the n_{sector} = 6 spider supports with w_{spider} = 7.0 mm width will completely obscure the region between the outer spacers of adjacent sextant segments including the nominal epoxy fillet width. The spiders will similarly obscure this region on one side of each of the twelvetant sectors such that only a small portion (1.2 mm for each twelvetant) of the unsupported overhang region outside the outermost spacer will be unobscured the other side of each of the twelvetant sectors. Including the spider obscuration and gaps between shells (for the twelvetants portion not covered by the spiders), the total on-axis obscuration will be

$$\varepsilon_{obscuration} = [n_{segs}\,(n_{spacers}-2)(w_{spacer}+w_{fillet}) + (n_{segs}-n_{sectors})(w_{gap}+2w_{spacer}+2w_{fillet}) + n_{sectors}\,w_{spider}] / (2\pi\, r_{lb}), \quad (5)$$

where $n_{spacers}$ = 5 is the number of spacers, $n_{segments}$ is the number of mirror segments as previously defined (i.e., 6 for the inner and 12 for the outer layers), n_{sector} = 6 is the number of spider legs (i.e. primary sectors), w_{spider} = 7.0 mm is the spider width and the epoxy fillet width (w_{fillet}) and spacer width (w_{spacer}) are as previously defined. The total obscuration for will range from 13-26%. The central spacers are positioned such that they are positioned at $\varphi_{o,i}$ = 360º (i+0.5)/n_{segs} in azimuth coordinates where i = 1,n_{segs} is the i^{th} segment, and the gap between the i and i+1 segments is at $\varphi_{gap,i}$ = 360º (i/n_{segs}). The outside spacers will be positioned such that the center of the spacer is a tangential distance of w_{oh} = 2.4 mm from the gap position. The other two spacers will be positioned at $\Delta\varphi_{o,i}$ = +- 360º/n_{segs} /($n_{spacers}$-1) from the central spacer. This geometry is illustrated in Figure 3.

Table 1: Overall optics design parameters

Parameter	Unit	Value	Uncertainty
Focal Length (F)	[mm]	10150[a]	
Innermost Shell Radius (r_{uo})	[mm]	54.418	
Outermost Shell Radius (r_{uo})	[mm]	191.221	
Shell Length (L)	[mm]	225.0	
Half Gap btw Upper/Lower Shell (g)	[mm]	2.0	
Epoxy Thickness (t_{epoxy})	[mm]	0.002	
Variable Gap (f_{gap})		1.3313[a]	
PSF performance (HPD)	[arcsec]	43	
Spacer Density (ρ_{spacer})	[g/cm^3]	1.88	±0.09
Epoxy Density (ρ_{epoxy})	[g/cm^3]	1.16	
Epoxy Per Spacer Length	[mg/cm]	2.5	+0.5,-1.0
Total Shells Per Module		130+3	
Total Mounted Segments		4680	
Total Cut/Coat Requirement		5200	
Total Slumping Requirement		4010	
Total Glass Sheet Requirement		2999	
Total Spacers		14256	

[a]In early 2009, the focal length was changed from 10140 mm to 10150 mm and as a result, the Variable Gap parameter was changed from 1.33 to 1.3313 in order to maintain the same shell geometry (within 0.01 mm).

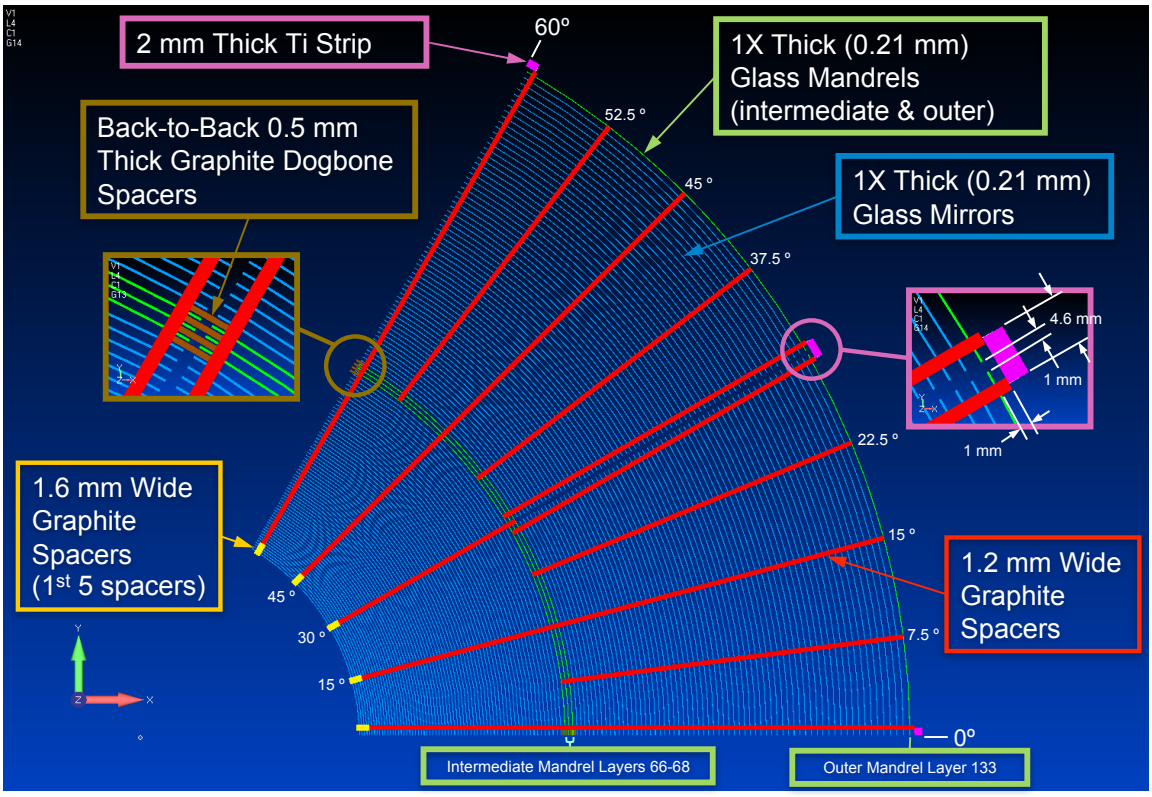

Figure 3: Close-up of top of the optic.

Table 2: Optics design details

Parameter	Unit	Inner	Interm.	Outer	Uncertainty
Layers		1-65	66-68	69-133	
Min Shell Radius (r_{uo})	[mm]	54.418	105.479	108.480	±0.003
Max Shell Radius (r_{uo})	[mm]	104.494	107.472	191.221	±0.003
Min Upper Shell Graze Angle (α_u)	[mrad]	1.342	2.601	2.675	±0.015
Max Upper Shell Graze Angle (α_u)	[mrad]	2.576	2.650	4.715	±0.015
Min Lower Shell Graze Angle (α_l)	[mrad]	4.026	7.803	8.025	±0.015
Max Lower Shell Graze Angle (α_l)	[mrad]	7.728	7.950	14.145	±0.015
Substrate Source		GSFC	GSFC	GSFC	
Glass Type		D263	D263	D263	
Glass Density (ρ_{glass})	[g/cm^3]	2.51	2.51	2.51	±0.01
Substrate Length (L_{glass})	[mm]	225.0	225.0	225.0	±0.2
Shell Length (L)	[mm]	225	225	225	
Sectors per (U/L) Shell (n_{seg})		6	6	12	
Gap btw Sectors (w_{gap})	[mm]	1.0	1.0	1.0	+0.5,-1.0
Sector Arclength Minimum	[mm]	54.9	107.3	54.7	
Sector Arclength Maximum	[mm]	107.7	111.9	99.4	
Sector Chord Length Minimum	[mm]	52.6	102.7	54.1	
Sector Chord Length Maximum	[mm]	103.9	106.9	98.3	
Total Mounted Segments		1560	72	3120	
Spares per layer per telescope		2	4	2	
Total Cut/Coat Requirement		1820	96	3380	
Slump + Cut Yield		90%	70%	85%	
Slump Pieces per Slump Mandrel		1.0	1.0	2.0	
Total Slumping Requirement		2022	137	1988	
Segments per Glass Sheet		2.0	2.0	1.0	
Total Glass Sheet Requirement		1011	69	1988	
Mirror Thickness (t_{glass})	[mm]	0.210	0.210	0.210	±0.006
Spacers per Sector (n_{spacer})		5	10	5	
Spacer Width (w_{spacer})	[mm]	1.2[a]	1.2	1.2	+0.0,-0.2
Epoxy Fillet Width (w_{fillet})	[mm]	1.0	1.0	1.0	+0.1,-0.3
Spacer + Epoxy Width	[mm]	2.2	2.6	2.2	
Distance btw Gap & Spacer (w_{oh})	[mm]	2.4	2.4	2.4	
Max. Spacer/Gap Obscuration [%]		26%	22%	23%	
Min. Spacer/Gap Obscuration [%]		13%	23%	13%	
Total Spacers		4752	360	9504	
Throughput Efficiency		92%[c]	0%[b]	92%[c]	+5,-7%

[a]1.6 mm for layers 1-5;

[b]Intermediate layers will likely have significant reflectivity, but are not included in baseline calculations for effective area.

[c]The finite PSF of the actual mirrors will reduce the on-axis effective area by 3-7% and affect the off-axis effective area by ±2%. This however is dependent on the exact shape and energy dependence of the PSF and not solely the HPD, and thus a slightly more conservative throughput value is given here.

Table 3: Optics mass estimates per optic (note that the uncertainty for the total mass per optic is given here simply as the linear sum of all uncertainty terms).

System	Unit	Estimate	Uncertainty
Glass Mirror Substrates	[kg]	21.32	±0.5
Graphite Spacers	[kg]	5.48	+0.5,-1.0
Epoxy	[kg]	0.67	+0.2,-0.3
Multilayer Coatings	[kg]	0.56	+0.2,-0.0
Inner Base Mandrel	[kg]	2.85	+0.0,-0.3
Intermediate Mandrel	[kg]	0.68	+0.2,-0.3
Outer Mandrel	[kg]	0.40	+0.2,-0.1
ZSpider & Mounts	[kg]	5.00	+0.2,-0.4
Thermal	[kg]	0.40	+0.3,-0.1
Total Mass per Optic	[kg]	37.36	+2.3,-2.7

3.4. Multilayer Design

3.4.1. Multilayer terminology

A multilayer is a stack of thin film of two different materials, deposited alternately on top of each other. To achieve the highest reflectivity the two materials must have a high density contrast and the materials are referred to as spacer, which is the low Z density material, and absorber, which is the high Z density material. One pair of spacer and absorber layers is called a bi-layer and has thickness d. The fraction of the absorber to the total thickness of the bi-layer is called $\Gamma = a_{absorber}/d$. The bi-layer progression of thicknesses of the multilayer is given by the power-law $d_i = a/(b+i)^c$, where *i* runs from 1 to the total number of bi-layers, N, that are in the stack. The thinnest layers are closest to the substrate, and the thickest at the top, where 1 is the very top bi-layer.

The power-law depth grading described above is used for layers N to 2. The gamma fraction, Γ, changes throughout the stack, starting at Γ_{high} at the bottom of the stack and finishing at Γ_{low} at the top.

The top layer, N=1, is treated slightly differently, and is designed to most efficiently reflect energies below the critical energy, related to the critical angle of total external reflection. Because the critical angle of total external reflection is higher for the denser materials, the top layer is designed to resemble a monolithic slab of Pt or W, with only a thin SiC or Si layer to protect the Pt, and instead of using the Γ of the stack (hereafter called Γ_{stack}), we use a different gamma, Γ_{top}, favoring a higher gamma. The bi-layer thickness used for the top layer is derived from the power-law formula, but the applied Γ is different.

3.4.2. Design constrains and optical constants

The multilayer recipes have been optimized using the Figure of Merit optimization program (Peter Mao et al, 1999).

We have divided the 133 shells of the optics into 10 mirror groups. The optimized parameters are:

D_{max} – Maximum bi-layer thickness

c – power-law index

N – Total number of bi-layers

The materials selected for our multilayer are Pt/C and W/Si. Due to coating restraints, Γ cannot be less than 0.3, and the total thickness of the stack cannot exceed 1.0 microns for W/Si and 0.6 microns for Pt/C and Pt/SiC.

The interfacial roughness for the materials are based on averages from experimental coatings, and are $\sigma_{Pt/C}$ = 4.5 Å, $\sigma_{W/Si}$ = 4.3 Å

The optical constants have been calculated theoretically and been experimentally verified. The optical constant files used for these optimizations are:

SiC_NIST_CPJ_081013

C_NIST_CPJ_081013

Pt_NIST_CPJ_081013

Si_NIST_CPJ_081013

W_NIST_CPJ_081013

The Figures below show the measured and theoretical curves for Pt. The theoretical curves were obtained from the National Institute of Standards and Technology.

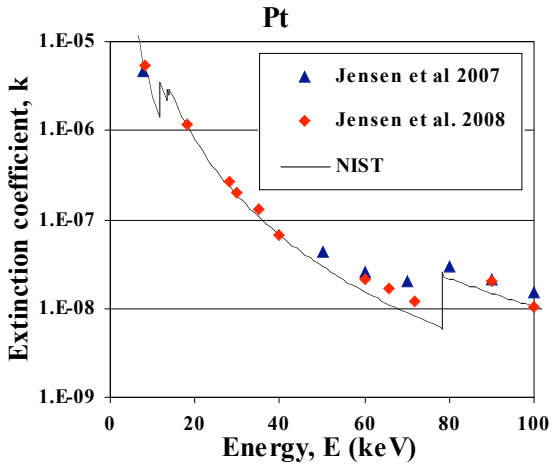

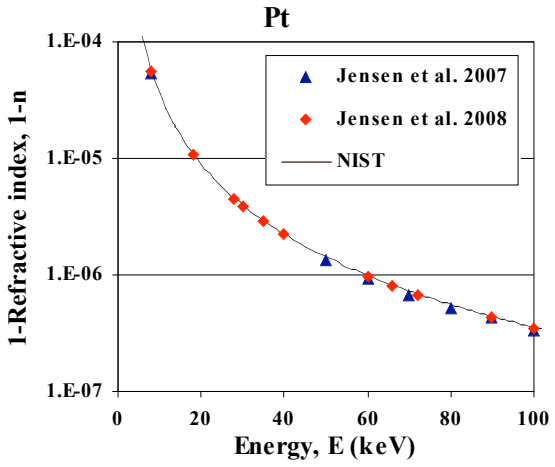

3.4.3. The Flight Recipes

Table 4. shows the 10 optimized recipes for flight optics FM1 and FM2. Table 5. Shows the recipes for optic FM0. Group 1 represents the inner mirrors and group 10 the outer.

Table 4: Multilayer Recipes for FM1/FM2

Group	Material	Angle [mrad]	Layer range	D_{min} [Å]	D_{max} [Å]	N	c	σ [Å]	Γ_{Top}	Γ_{high}	D_{stack} [μm]
1	Pt/C	1.34 - 1.52	1 - 12	29	133.66	145	0.245	4.5	0.7	0.45	0.558
2	Pt/C	- 1.73	13 – 24	29	131.58	145	0.228	4.5	0.7	0.45	0.547
3	Pt/C	- 1.96	25 – 36	29	129.56	145	0.234	4.5	0.7	0.45	0.551
4	Pt/C	- 2.22	37 – 49	29	121.84	145	0.214	4.5	0.7	0.45	0.537
5	Pt/C	- 2.52	50 – 62	29	109.50	145	0.225	4.5	0.7	0.45	0.541
6	Pt/C	- 2.85	63 – 76	29	107.50	145	0.225	4.5	0.7	0.45	0.541
7	Pt/C	- 3.23	77 – 89	29	102.75	145	0.212	4.5	0.7	0.45	0.534
8	W/Si	- 3.67	90 – 104	25.0	95.228	291	0.238	4.3	0.8	0.38	0.955
9	W/Si	- 4.16	105 – 118	25.0	83.942	291	0.220	4.3	0.8	0.38	0.934
10	W/Si	- 4.72	119 - 133	25.0	74.471	291	0.190	4.3	0.8	0.38	0.902

Note that for groups 8 – 10, Γ_{Top} is equal to 0.8. The W thickness is thus $\Gamma_{Top}*d_{max}$ but since $(1-\Gamma_{Top})*d_{max}$ < 25 AA, the top Si layer has been fixed at 25 AA.

Table 5: Multilayer Recipes for FM0.

Group	Material	Angle [mrad]	Layer range	D_{min} [Å]	D_{max} [Å]	N	c	σ [Å]	Γ_{Top}	Γ_{high}	D_{stack} [μm]
1	Pt/SiC	1.34 - 1.52	1 - 12	31.7	128.125	150	0.245	4.5	0.7	0.45	0.631
2	Pt/SiC	- 1.73	13 – 24	30.5	120.935	150	0.228	4.5	0.7	0.45	0.611
3	Pt/SiC	- 1.96	25 – 36	29.0	119.500	155	0.234	4.5	0.7	0.45	0.592
4	Pt/SiC	- 2.22	37 – 49	29.0	118.188	155	0.214	4.5	0.7	0.45	0.578
5	Pt/SiC	- 2.52	50 – 62	29.0	107.750	155	0.225	4.5	0.7	0.45	0.575
6	Pt/SiC	- 2.85	63 – 76	29.0	103.250	155	0.225	4.5	0.7	0.45	0.586
7	Pt/SiC	- 3.23	77 – 89	29.0	98.750	155	0.212	4.5	0.7	0.45	0.577
8	W/Si	- 3.67	90– 104	25.0	95.228	291	0.238	4.3	0.8	0.38	0.955
9	W/Si	- 4.16	105 – 118	25.0	83.942	291	0.220	4.3	0.8	0.38	0.934
10	W/Si	- 4.72	119 - 133	25.0	74.471	291	0.190	4.3	0.8	0.38	0.902

Note that for groups 8 – 10, Γ_{Top} is equal to 0.8. The W thickness is thus $\Gamma_{Top}*d_{max}$ but since $(1-\Gamma_{Top})*d_{max}$ < 25 AA, the top Si layer has been fixed at 25 AA.

4. Design Uncertainties

Based on the mechanical description in Section 3, the design uncertainties for relevant optics parameters are detailed in Table 1 and Table 2.

4.1. Spacers

Based on the vendor tolerance specification, the uncertainty in the spacer width is δw_{spacer} = ±0.02 mm (i.e., ~2%). Six spacers from the first set of spacers we received from the vendor were measured to be within the tolerance specification with an average measured width of 1.22 mm and a measurement accuracy of ±0.01 mm.

Carbone-DS4 is the name of the graphite that is baselined for the spacers. It is manufactured by Carbone of America and machined to the required spacer size by Industrial Graphite. The graphite was chosen to closely match the CTE of the D263 glass substrates. The density has been measured to be 1.88±0.02 g/cm^3, based on 101 spacers measured in units of 10 to 11 spacers. Given that the density may vary from batch to batch we estimate the uncertainty in the graphite density to be ±0.09 g/cm^3 (i.e. 5%).

4.2. Epoxy

Since the epoxy is manually applied, we expect there will be variation in the individual fillet widths. The estimate of the average epoxy fillet ('squish-out') near the spacers, w_{fillet} = 1.0 mm (i.e. 0.5 mm on each side of the spacer), is based of both X-ray and microscope measurements of the bondline width achieved with the baseline method of applying the EP-30 epoxy. We estimate that the uncertainty in the fillet width for NuSTAR will be δw_{fillet} = [+0.1 mm, -0.3 mm].

Based on results from the epoxy development program, the current best estimate for the average mass of epoxy per unit glass/graphite bond length is 2.5 mg/cm. The uncertainty is epoxy mass is estimated to be +0.5,-1.0 mg/cm.

4.3. Glass

The specification for the average gap between adjacent mirror segments (w_{gap} = 1 mm gap) is based on the specification for the substrate cutting templates. Measurements of cut shells indicate that the average arclengths of the cut shells are slightly smaller than the cut specifications (i.e., leading to a slightly larger average gap), however, it is expected that this will only have a positive impact on the mass margin (i.e. less mass). Only one side of each twelvetant substrate will provide effective area near the gap between adjacent segments with the other side covered by the spider structure. Thus the twelvetants will be aligned to the 1 mm gap tolerance in the exposed region such that any extra gap in the region covered by the spider will not cause any decrease in effective area. The estimated uncertainty in the average gap of +0.5 mm, -1.0 mm provides sufficient tolerance in the substrate cut dimensions to assure high cut yields with no undesirable impact on the mass or effective area margins. Figure 4 and Figure 5 show the measured deviations from the cut geometry prescriptions for arc-length.

The uncertainty in average substrate length is expected to be $\delta L = \pm 0.2$ mm. The axial length was measured for a sample of 1448 substrates with 80% of them within the measurement accuracy of ±0.25 mm and less than 7% with deviations of more than ±0.75 mm from the design value of 225 mm.

The glass density (2.51 g/cm^3) and thickness (0.210 mm) is based on standard Schott D263 microsheets. While the density is expected to be very uniform with little uncertainty (~0.01 g/cm^3), the uncertainty in the thickness is quoted by Schott to be ±0.025 mm. We have measured the thickness uniformity of individual sheets to be ~0.003 mm throughout the sheet but slowly changing and ~<0.001 mm in the draw direction (which is chosen to be the axial slump direction). In terms of performance verification with surface metrology on the back surface of the mirrors, the thickness uncertainty poses a negligible contribution. Sheets from the same box (100 sheets per box) which come from the same glass production run show similarly low (<~0.005 mm) distribution in thickness. The thickness uncertainty quoted by Schott is a maximum deviation for any sheet from any production run. For the purpose of mass calculation, we are only concerned with the average thickness and density; thus, we estimate that the uncertainty in the mass estimate of the glass is 3%. The thickness uncertainty will have an extremely small affect (<<1%) on the off-axis effective area due to vignetting.

The mass of 23 flight mirror (from layers 1, 9 and 27) was measured to be -1.5±0.5 relative to the specified mass based on the cut prescriptions and density and thickness specifications. While we do not have independent measurements of the glass thickness and density, these measurements indicate that density and thickness values specified in this document must be close to their actual values.

4.4. Structural

As previously mentioned, the spider supports will be aligned with to completely obscure the region between the outer spacers of adjacent sextant segments (and one side of each twelvetant segment) including the nominal epoxy fillet width. The tolerance of the spider width will be small (<±0.1 mm). Thus the throughput near the spiders will only be negatively affected by excessive epoxy fillets (<1.0 mm).

The baseline design for the structural hardware (e.g., inner, intermediate and outer mandrels; mounting spider and related components) is estimated to have a mass uncertainty of +10%, -20%.

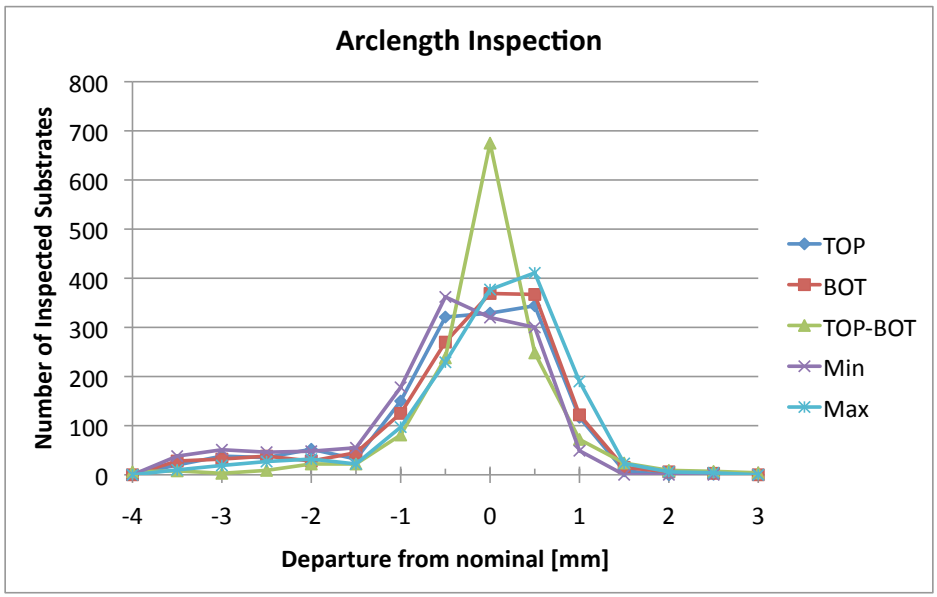

Figure 4: Histogram of measured deviation of the mirror arc-length measurement from the cut shell specifications for 1448 mirrors. Top (Bot) refers to the arc-length measured at the top (bottom) of the mirror, 'Top-Bot' is the difference between the top and bottom measurement for each mirror, and min (max) is the minimum (maximum) value of the top and bottom measurements.

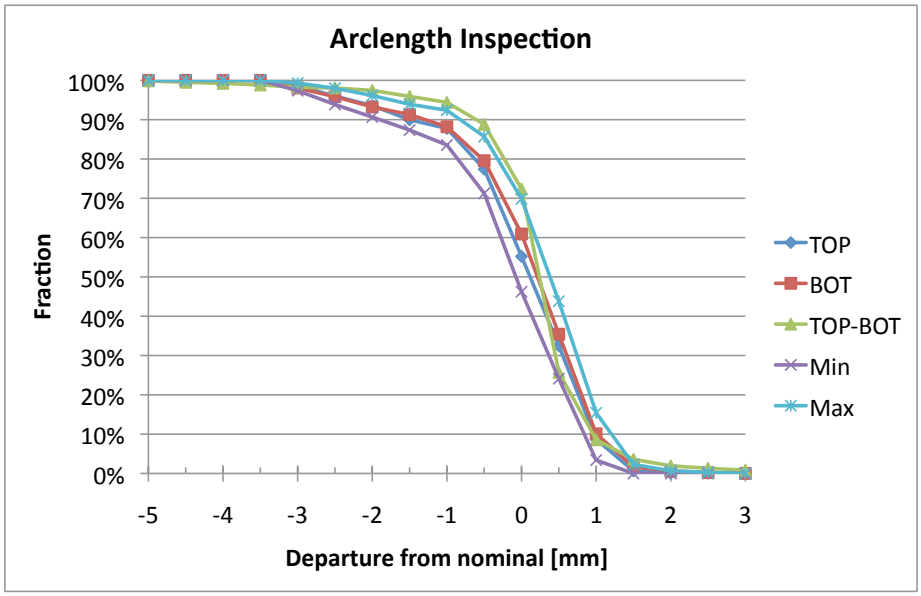

Figure 5: Integrated fraction of mirrors versus deviation from cut specification. See **Figure 4** caption for description of data labels.

5. Current Best Estimate Performance

The effective area is calculated using a raytrace program that includes the optics geometry, structural obscuration (vignetting, spacers, epoxy fillet, etc.), multilayer reflectivity and a model of the expected scatter from the mirrors due to figure error. Based on the mechanical description in Section 3, the current best estimate of the effective area for each telescope coated with FM1/FM2 multilayer recipes, as a function

of energy and off-axis viewing angles 3 arcminutes and 6 arcminutes is plotted in Figure 6. The plot includes the reduction in effective area due to the thermal blankets and the aperture stop. The intermediate transition layers 66-68 are expected to be comprised of multilayer coated mirrors that will provide additional effective area, but are not included in the effective area calculations.

The most recent response files can be found at

http://www.nustar.caltech.edu/for-astronomers/simulations

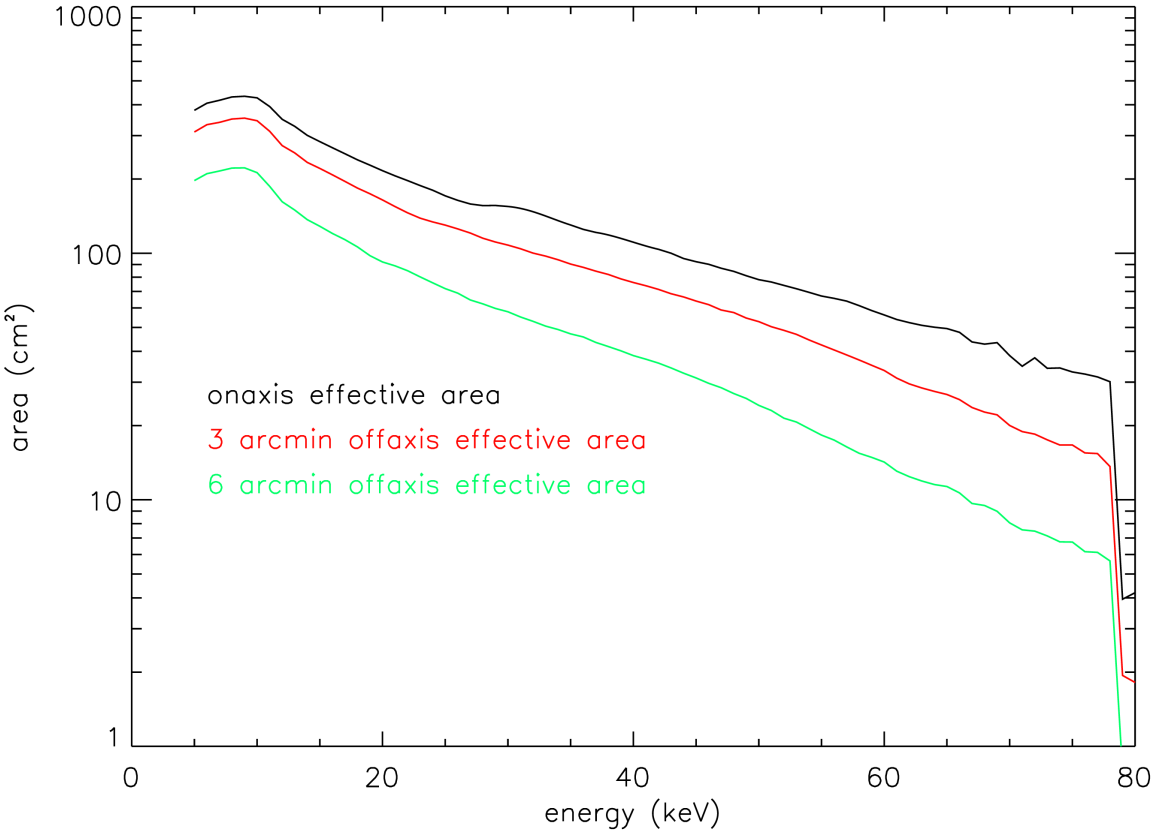

Figure 6: Effective Area as a function of energy for on- and off-axis photons for one telescope. Area includes reduction in area due to thermal blankets, the presence of aperture stop and scattering due to figure errors in the mirrors. The multilayer recipes used here are for FM1 and FM2.

Table 6: Mirror segment geometry for intermediate transition layers

Layer	α_u	α_l	r_{ut}	r_{ub}	r_{lt}	r_{lb}	n_{segs}	w_{gap}	s_{ut}	s_{ub}	s_{lt}	s_{lb}
	[mrad]	[mrad]	[mm]	[mm]	[mm]	[mm]		[mm]	[mm]	[mm]	[mm]	[mm]
66	2.598	7.794	105.772	105.188	105.167	103.413	6	1.0	109.76	109.15	109.13	107.29
67	2.622	7.866	106.768	106.178	106.157	104.387	6	1.0	110.81	110.19	110.17	108.31
68	2.647	7.941	107.771	107.175	107.154	105.367	6	1.0	111.86	111.23	111.21	109.34

Table 7: Mirror segment geometry for inner layers

Layer	α_u	α_l	r_{ut}	r_{ub}	r_{lt}	r_{lb}	n_{segs}	w_{gap}	s_{ut}	s_{ub}	s_{lt}	s_{lb}
	[mrad]	[mrad]	[mm]	[mm]	[mm]	[mm]		[mm]	[mm]	[mm]	[mm]	[mm]
1	1.340	4.020	54.569	54.267	54.257	53.352	6	1.0	56.14	55.83	55.82	54.87
2	1.355	4.065	55.185	54.881	54.870	53.955	6	1.0	56.79	56.47	56.46	55.50
3	1.371	4.113	55.805	55.497	55.486	54.560	6	1.0	57.44	57.12	57.10	56.14
4	1.386	4.158	56.431	56.119	56.108	55.172	6	1.0	58.09	57.77	57.76	56.78
5	1.402	4.206	57.061	56.745	56.734	55.788	6	1.0	58.75	58.42	58.41	57.42
6	1.417	4.251	57.695	57.377	57.365	56.409	6	1.0	59.42	59.08	59.07	58.07
7	1.433	4.299	58.334	58.012	58.000	57.033	6	1.0	60.09	59.75	59.74	58.72
8	1.449	4.347	58.978	58.652	58.640	57.662	6	1.0	60.76	60.42	60.41	59.38
9	1.465	4.395	59.627	59.297	59.285	58.297	6	1.0	61.44	61.10	61.08	60.05
10	1.481	4.443	60.281	59.947	59.936	58.936	6	1.0	62.13	61.78	61.76	60.72
11	1.497	4.491	60.938	60.602	60.590	59.579	6	1.0	62.81	62.46	62.45	61.39
12	1.513	4.539	61.602	61.262	61.250	60.228	6	1.0	63.51	63.15	63.14	62.07
13	1.530	4.590	62.270	61.926	61.914	60.881	6	1.0	64.21	63.85	63.84	62.75
14	1.546	4.638	62.943	62.595	62.583	61.539	6	1.0	64.91	64.55	64.54	63.44
15	1.563	4.689	63.622	63.270	63.258	62.203	6	1.0	65.62	65.26	65.24	64.14
16	1.579	4.737	64.305	63.949	63.937	62.871	6	1.0	66.34	65.97	65.95	64.84
17	1.596	4.788	64.993	64.633	64.621	63.543	6	1.0	67.06	66.68	66.67	65.54
18	1.613	4.839	65.685	65.323	65.310	64.221	6	1.0	67.79	67.41	67.39	66.25
19	1.631	4.893	66.384	66.018	66.004	64.904	6	1.0	68.52	68.13	68.12	66.97
20	1.648	4.944	67.088	66.718	66.704	65.592	6	1.0	69.25	68.87	68.85	67.69
21	1.665	4.995	67.796	67.422	67.408	66.284	6	1.0	70.00	69.60	69.59	68.41
22	1.683	5.049	68.511	68.133	68.119	66.983	6	1.0	70.74	70.35	70.33	69.14
23	1.700	5.100	69.230	68.848	68.834	67.687	6	1.0	71.50	71.10	71.08	69.88
24	1.718	5.154	69.955	69.569	69.555	68.395	6	1.0	72.26	71.85	71.84	70.62
25	1.736	5.208	70.685	70.295	70.281	69.109	6	1.0	73.02	72.61	72.60	71.37
26	1.754	5.262	71.420	71.026	71.012	69.828	6	1.0	73.79	73.38	73.36	72.12
27	1.772	5.316	72.161	71.763	71.748	70.552	6	1.0	74.57	74.15	74.13	72.88
28	1.791	5.373	72.907	72.505	72.490	71.281	6	1.0	75.35	74.93	74.91	73.65
29	1.809	5.427	73.660	73.252	73.238	72.017	6	1.0	76.14	75.71	75.69	74.42
30	1.828	5.484	74.418	74.006	73.992	72.758	6	1.0	76.93	76.50	76.48	75.19
31	1.847	5.541	75.181	74.765	74.750	73.504	6	1.0	77.73	77.29	77.28	75.97
32	1.866	5.598	75.949	75.529	75.514	74.255	6	1.0	78.53	78.09	78.08	76.76
33	1.885	5.655	76.724	76.300	76.285	75.012	6	1.0	79.35	78.90	78.89	77.55
34	1.904	5.712	77.504	77.076	77.061	75.775	6	1.0	80.16	79.71	79.70	78.35
35	1.923	5.769	78.290	77.858	77.842	76.544	6	1.0	80.99	80.53	80.52	79.16
36	1.942	5.826	79.081	78.645	78.629	77.318	6	1.0	81.81	81.36	81.34	79.97
37	1.962	5.886	79.880	79.438	79.423	78.098	6	1.0	82.65	82.19	82.17	80.78
38	1.982	5.946	80.683	80.237	80.221	78.883	6	1.0	83.49	83.02	83.01	81.61
39	2.002	6.006	81.492	81.042	81.026	79.674	6	1.0	84.34	83.87	83.85	82.43
40	2.022	6.066	82.308	81.854	81.837	80.472	6	1.0	85.19	84.72	84.70	83.27
41	2.042	6.126	83.130	82.670	82.654	81.276	6	1.0	86.05	85.57	85.56	84.11
42	2.062	6.186	83.958	83.494	83.478	82.086	6	1.0	86.92	86.43	86.42	84.96
43	2.083	6.249	84.791	84.323	84.306	82.900	6	1.0	87.79	87.30	87.29	85.81
44	2.103	6.309	85.632	85.158	85.142	83.722	6	1.0	88.67	88.18	88.16	86.67
45	2.124	6.372	86.478	86.000	85.983	84.549	6	1.0	89.56	89.06	89.04	87.54
46	2.145	6.435	87.330	86.848	86.831	85.383	6	1.0	90.45	89.95	89.93	88.41
47	2.166	6.498	88.189	87.701	87.684	86.222	6	1.0	91.35	90.84	90.82	89.29
48	2.187	6.561	89.054	88.562	88.544	87.068	6	1.0	92.26	91.74	91.72	90.18
49	2.209	6.627	89.926	89.428	89.411	87.920	6	1.0	93.17	92.65	92.63	91.07
50	2.230	6.690	90.804	90.302	90.284	88.779	6	1.0	94.09	93.56	93.55	91.97
51	2.252	6.756	91.688	91.182	91.164	89.644	6	1.0	95.02	94.49	94.47	92.87
52	2.274	6.822	92.580	92.068	92.050	90.515	6	1.0	95.95	95.41	95.39	93.79
53	2.296	6.888	93.477	92.961	92.942	91.393	6	1.0	96.89	96.35	96.33	94.71
54	2.318	6.954	94.382	93.860	93.842	92.277	6	1.0	97.84	97.29	97.27	95.63
55	2.341	7.023	95.293	94.767	94.748	93.168	6	1.0	98.79	98.24	98.22	96.57
56	2.363	7.089	96.211	95.679	95.660	94.065	6	1.0	99.75	99.19	99.18	97.50
57	2.386	7.158	97.135	96.599	96.579	94.969	6	1.0	100.72	100.16	100.14	98.45
58	2.409	7.227	98.067	97.525	97.506	95.880	6	1.0	101.70	101.13	101.11	99.40
59	2.432	7.296	99.006	98.458	98.439	96.797	6	1.0	102.68	102.11	102.09	100.37
60	2.455	7.365	99.951	99.399	99.379	97.722	6	1.0	103.67	103.09	103.07	101.33
61	2.478	7.434	100.904	100.346	100.326	98.654	6	1.0	104.67	104.08	104.06	102.31
62	2.502	7.506	101.862	101.300	101.280	99.591	6	1.0	105.67	105.08	105.06	103.29
63	2.526	7.578	102.829	102.261	102.241	100.536	6	1.0	106.68	106.09	106.07	104.28
64	2.550	7.650	103.803	103.229	103.209	101.487	6	1.0	107.70	107.10	107.08	105.28
65	2.574	7.722	104.784	104.204	104.184	102.446	6	1.0	108.73	108.12	108.10	106.28

Table 8: Mirror segment geometry for outer layers

Layer	α_u	α_l	r_{ut}	r_{ub}	r_{lt}	r_{lb}	n_{segs}	w_{gap}	s_{ut}	s_{ub}	s_{lt}	s_{lb}
	[mrad]	[mrad]	[mm]	[mm]	[mm]	[mm]		[mm]	[mm]	[mm]	[mm]	[mm]
69	2.672	8.016	108.781	108.179	108.158	106.354	12	1.0	55.96	55.64	55.63	54.69
70	2.697	8.091	109.799	109.193	109.171	107.351	12	1.0	56.49	56.17	56.16	55.21
71	2.722	8.166	110.824	110.212	110.190	108.353	12	1.0	57.03	56.71	56.70	55.73
72	2.747	8.241	111.857	111.239	111.217	109.363	12	1.0	57.57	57.24	57.23	56.26
73	2.773	8.319	112.898	112.274	112.252	110.380	12	1.0	58.11	57.79	57.77	56.79
74	2.799	8.397	113.946	113.316	113.294	111.404	12	1.0	58.66	58.33	58.32	57.33
75	2.825	8.475	115.003	114.367	114.345	112.438	12	1.0	59.22	58.88	58.87	57.87
76	2.851	8.553	116.067	115.425	115.402	113.478	12	1.0	59.77	59.44	59.42	58.42
77	2.877	8.631	117.139	116.491	116.468	114.526	12	1.0	60.33	59.99	59.98	58.97
78	2.904	8.712	118.218	117.564	117.541	115.581	12	1.0	60.90	60.56	60.54	59.52
79	2.930	8.790	119.306	118.646	118.623	116.645	12	1.0	61.47	61.12	61.11	60.08
80	2.957	8.871	120.402	119.736	119.713	117.717	12	1.0	62.04	61.69	61.68	60.64
81	2.984	8.952	121.506	120.834	120.810	118.796	12	1.0	62.62	62.27	62.26	61.20
82	3.012	9.036	122.618	121.940	121.916	119.883	12	1.0	63.20	62.85	62.84	61.77
83	3.039	9.117	123.738	123.054	123.030	120.978	12	1.0	63.79	63.43	63.42	62.34
84	3.067	9.201	124.867	124.177	124.152	122.082	12	1.0	64.38	64.02	64.01	62.92
85	3.095	9.285	126.004	125.308	125.283	123.194	12	1.0	64.98	64.61	64.60	63.50
86	3.123	9.369	127.149	126.447	126.422	124.314	12	1.0	65.58	65.21	65.19	64.09
87	3.151	9.453	128.303	127.595	127.569	125.442	12	1.0	66.18	65.81	65.80	64.68
88	3.180	9.540	129.466	128.750	128.725	126.578	12	1.0	66.79	66.41	66.40	65.28
89	3.209	9.627	130.637	129.915	129.889	127.723	12	1.0	67.40	67.02	67.01	65.88
90	3.238	9.714	131.817	131.089	131.063	128.877	12	1.0	68.02	67.64	67.62	66.48
91	3.267	9.801	133.006	132.270	132.244	130.039	12	1.0	68.64	68.26	68.24	67.09
92	3.296	9.888	134.203	133.461	133.435	131.210	12	1.0	69.27	68.88	68.87	67.70
93	3.326	9.978	135.409	134.661	134.634	132.389	12	1.0	69.90	69.51	69.49	68.32
94	3.356	10.068	136.625	135.869	135.843	133.577	12	1.0	70.54	70.14	70.13	68.94
95	3.386	10.158	137.849	137.087	137.060	134.774	12	1.0	71.18	70.78	70.76	69.57
96	3.416	10.248	139.082	138.314	138.286	135.981	12	1.0	71.82	71.42	71.41	70.20
97	3.447	10.341	140.325	139.549	139.522	137.195	12	1.0	72.47	72.07	72.05	70.84
98	3.477	10.431	141.576	140.794	140.766	138.419	12	1.0	73.13	72.72	72.70	71.48
99	3.508	10.524	142.837	142.047	142.019	139.651	12	1.0	73.79	73.38	73.36	72.12
100	3.540	10.620	144.107	143.311	143.282	140.893	12	1.0	74.45	74.04	74.02	72.77
101	3.571	10.713	145.387	144.583	144.555	142.144	12	1.0	75.12	74.70	74.69	73.43
102	3.603	10.809	146.676	145.866	145.837	143.405	12	1.0	75.80	75.38	75.36	74.09
103	3.635	10.905	147.975	147.157	147.128	144.674	12	1.0	76.48	76.05	76.04	74.75
104	3.667	11.001	149.284	148.458	148.429	145.954	12	1.0	77.16	76.73	76.72	75.42
105	3.699	11.097	150.601	149.769	149.739	147.242	12	1.0	77.85	77.42	77.40	76.10
106	3.732	11.196	151.929	151.089	151.059	148.540	12	1.0	78.55	78.11	78.09	76.78
107	3.765	11.295	153.267	152.419	152.389	149.848	12	1.0	79.25	78.81	78.79	77.46
108	3.798	11.394	154.614	153.760	153.729	151.166	12	1.0	79.96	79.51	79.49	78.15
109	3.831	11.493	155.972	155.110	155.079	152.493	12	1.0	80.67	80.22	80.20	78.85
110	3.865	11.595	157.340	156.470	156.439	153.830	12	1.0	81.38	80.93	80.91	79.55
111	3.898	11.694	158.718	157.840	157.809	155.178	12	1.0	82.10	81.65	81.63	80.25
112	3.933	11.799	160.105	159.221	159.189	156.534	12	1.0	82.83	82.37	82.35	80.96
113	3.967	11.901	161.503	160.611	160.579	157.901	12	1.0	83.56	83.10	83.08	81.68
114	4.002	12.006	162.912	162.012	161.980	159.278	12	1.0	84.30	83.83	83.81	82.40
115	4.036	12.108	164.331	163.423	163.391	160.666	12	1.0	85.04	84.57	84.55	83.12
116	4.071	12.213	165.761	164.845	164.812	162.065	12	1.0	85.79	85.31	85.30	83.86
117	4.107	12.321	167.201	166.277	166.244	163.472	12	1.0	86.55	86.06	86.05	84.59
118	4.143	12.429	168.652	167.720	167.687	164.890	12	1.0	87.31	86.82	86.80	85.34
119	4.178	12.534	170.114	169.174	169.141	166.320	12	1.0	88.07	87.58	87.56	86.09
120	4.215	12.645	171.586	170.638	170.604	167.759	12	1.0	88.84	88.35	88.33	86.84
121	4.251	12.753	173.069	172.113	172.079	169.209	12	1.0	89.62	89.12	89.10	87.60
122	4.288	12.864	174.563	173.599	173.564	170.670	12	1.0	90.40	89.90	89.88	88.36
123	4.325	12.975	176.070	175.096	175.062	172.142	12	1.0	91.19	90.68	90.66	89.13
124	4.362	13.086	177.586	176.604	176.569	173.625	12	1.0	91.98	91.47	91.45	89.91
125	4.399	13.197	179.114	178.124	178.089	175.120	12	1.0	92.78	92.27	92.25	90.69
126	4.437	13.311	180.653	179.655	179.619	176.624	12	1.0	93.59	93.07	93.05	91.48
127	4.475	13.425	182.203	181.197	181.161	178.140	12	1.0	94.40	93.87	93.86	92.27
128	4.514	13.542	183.766	182.750	182.714	179.667	12	1.0	95.22	94.69	94.67	93.07
129	4.552	13.656	185.339	184.315	184.278	181.206	12	1.0	96.04	95.51	95.49	93.88
130	4.591	13.773	186.924	185.892	185.855	182.756	12	1.0	96.87	96.33	96.31	94.69
131	4.631	13.893	188.521	187.479	187.442	184.316	12	1.0	97.71	97.16	97.14	95.51
132	4.670	14.010	190.130	189.080	189.042	185.890	12	1.0	98.55	98.00	97.98	96.33
133	4.710	14.130	191.751	190.691	190.653	187.474	12	1.0	99.40	98.85	98.83	97.16